

## Supporting Information

### Monitoring Cooperative Binding using Electrochemical DNA-Based Sensors

Florika C. Macazo,<sup>†</sup> Richard L. Karpel,<sup>†</sup> and Ryan J. White<sup>†\*</sup>

<sup>†</sup> Department of Chemistry and Biochemistry, University of Maryland Baltimore County, Baltimore, Maryland 2125

#### Table of Contents

##### Derivation of Langmuir Isotherm to Describe Binding to (dT)<sub>7</sub> Probes

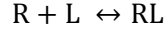
**Figure S1.** Direct comparison of the DNA probe surface densities obtained using the “backfill” and “insertion” sensor modification methods.

**Figure S2.** Direct comparison of the percent signal changes and apparent binding affinities ( $K_{Dapp}$ ) from data acquired using the “backfill” and “insertion” sensor modification methods.

**Figure S3.** Direct comparison of the current densities produced by the (dT)<sub>n</sub> E-DNA sensors at low (20 mM NaCl) and high (500 mM NaCl) salt concentrations.

## Derivation of Langmuir Isotherm to Describe Binding to (dT)<sub>7</sub> Probes

We can write an equilibrium expression for the interaction between our surface-bound d(T)<sub>7</sub> (R) and the g32p (L) assuming single, non-interacting binding sites as :



where the equilibrium association constant ( $K_a = M^{-1}$ ) and dissociation constant ( $K_d = M$ ) are given as:

$$K_a = \frac{[RL]}{[R][L]} \text{ and } K_d = \frac{1}{K_a} = \frac{[R][L]}{[RL]}$$

We also define the total concentration of d(T)<sub>7</sub> and g32p ( $[R]_o$  and  $[L]_o$ ) as

$$[R]_o = [R] + [RL] \text{ and } [L]_o = [L] + [RL]$$

where  $[R]$  and  $[L]$  represent unbound or free receptor and ligand. With these definitions we can also define the fraction of occupied binding sites ( $\beta$ ) and unoccupied sites ( $\alpha$ ) as

$$\beta = \frac{[RL]}{[R]_o} \text{ and } \alpha = \frac{[R]}{[R]_o}$$

$$\alpha + \beta = 1$$

Rearranging in terms of amount of receptor:ligand complex  $[RL]$ , and making the assumption that ligand binding to receptor does not appreciably change free ligand concentration ( $[L]_o \approx [L]$ ) we arrive at expressions for  $\alpha$  and  $\beta$  in terms of the  $K_a$  or  $K_d$ .

$$[RL] = K_a [R][L]$$

$$\alpha = \frac{[R]}{[R]_o} = \frac{[R]}{[R] + [RL]} = \frac{[R]}{[R] + K_a [R][L]}$$

$$\alpha = \frac{1}{1 + K_a [L]}$$

$$\beta = \frac{[RL]}{[R]_o} = \frac{[RL]}{[R] + [RL]} = \frac{K_a [R][L]}{[R] + K_a [R][L]}$$

$$\beta = \frac{K_a [L]}{1 + K_a [L]}$$

Finally, rewriting  $\beta$  in terms of  $K_d$  and sensor signal we arrive at the isotherm used in our manuscript.

$$S = S_{\max} \frac{[L]}{K_{Dapp} + [L]} \text{ and } \frac{S}{S_{\max}} = \beta$$

where  $S$  is sensor signal at  $[L]$  and  $S_{\max}$  is signal at saturating ligand concentration. This derivation is adapted from reference 1.<sup>1</sup>

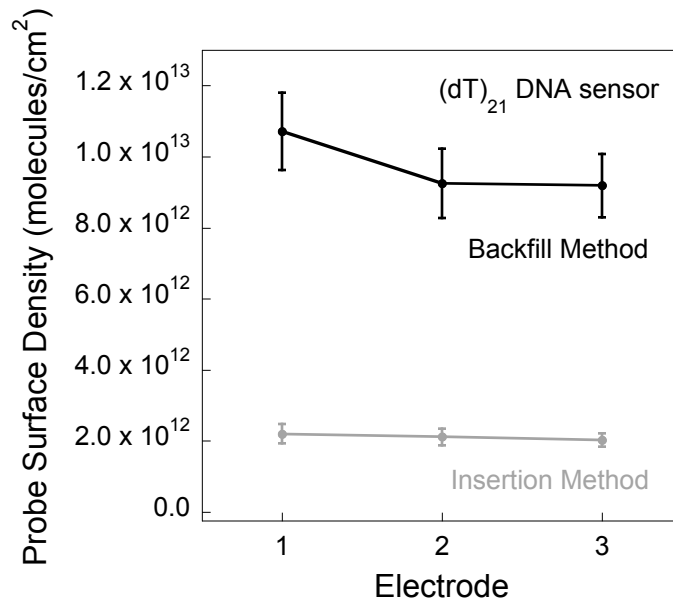


**FIGURE S1. The fabricated E-DNA sensor exhibit significantly lower surface coverage using the “insertion” sensor modification method as determined by chronocoulometry.** E-DNA sensors modified with (dT)<sub>21</sub> DNA probes are fabricated using both the “backfill” and “insertion” sensor modification methods as described in Figure S1. We quantified the surface density of (dT)<sub>21</sub> DNA by calculating the number of cationic redox molecules (hexaammineruthenium(III) chloride) that are associated or electrostatically trapped at the anionic DNA phosphate backbone via chronocoulometry. The “insertion” method allows the “insertion” of DNA molecules into the “defect” sites of the pre-formed passivating layer of 6-mercaptohexanol on the gold electrode surface, which results in a more uniform distribution of the DNA molecules on the pre-passivated sensor surface.<sup>2</sup> Consequently, our data is consistent with this report, as it shows lower calculated probe surface densities for the sensors modified using this method (gray curve). In contrast, the “backfill” method is expected to yield higher probe surface densities (e.g. DNA aggregation), which is clearly demonstrated in Figure S2 (black curve).

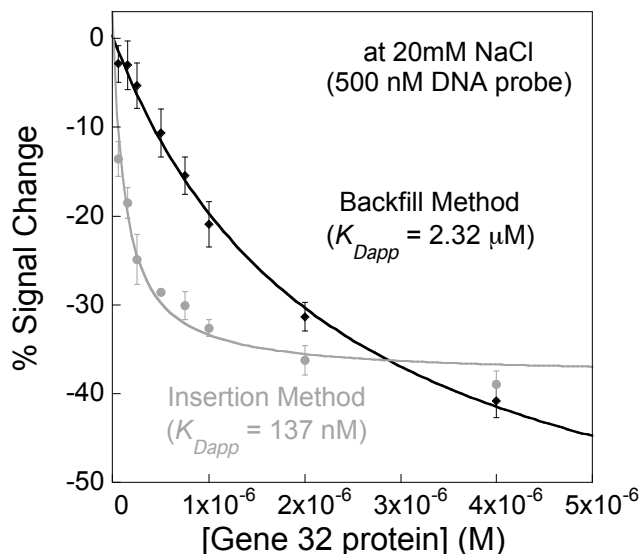


**FIGURE S2. The fabricated E-DNA sensor shows greater apparent binding affinity ( $K_{Dapp}$ ), as well as higher reproducibility using the “insertion” sensor modification method in contrast to the “backfill” method.** E-DNA sensors modified with a linear DNA probe are fabricated using both the “backfill” and “insertion” sensor modification methods. In the “backfill” method, the gold electrode surface is first incubated with 500 nM linear DNA probe, followed by “backfilling” with 6-mercaptohexanol that acts as a passivating layer. In the “insertion” method, a passivating layer of 6-mercaptohexanol is first formed across the gold electrode surface, followed by the addition of 500 nM linear DNA probe, which allows the “insertion” of the DNA molecules into the “defect” sites of the pre-formed passivating layer. Upon binding of target, a “signal-off” sensor is created, resulting in a decrease in the voltammetric peak current, expressed as a percent signal change in the binding curve. The E-DNA sensors demonstrate a significant increase in the apparent binding affinity using the “insertion” method ( $K_{Dapp} = 137 \text{ nM}$ ), as opposed to the lower apparent binding affinity obtained using the “backfill” method ( $K_{Dapp} = 2.32 \mu\text{M}$ ). In addition, higher reproducibility in the results is observed from using the “insertion” method, which may be a consequence of a more uniform distribution of the DNA molecules on the pre-passivated sensor surface.<sup>2</sup> Thus, the “insertion” sensor modification method is employed in all of the experiments reported in this manuscript.

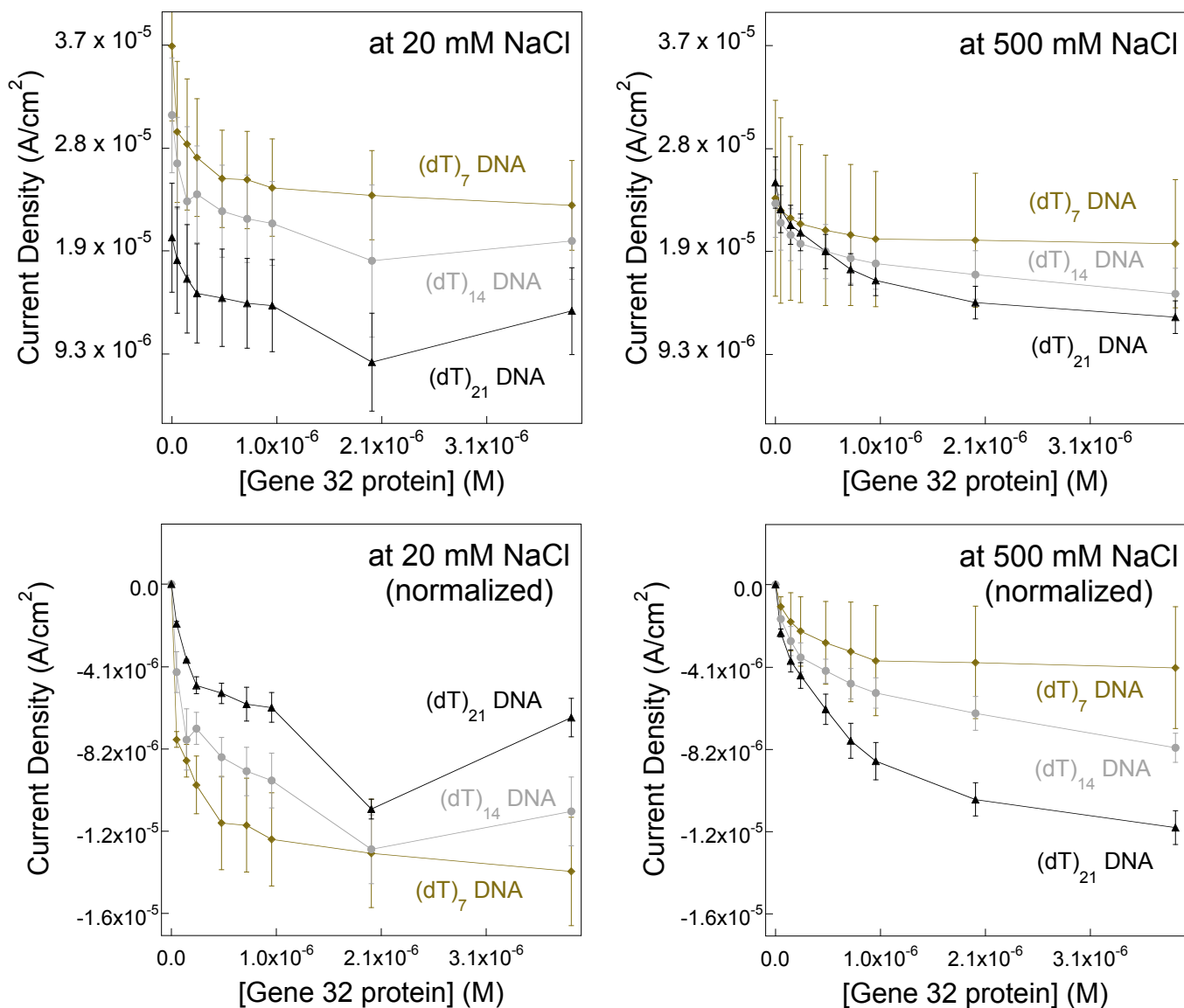


**FIGURE S3. The current densities measured using the (dT)<sub>n</sub> E-DNA sensors show quantitative dependence on both the ionic strength and DNA probe length.** E-DNA sensors modified with (dT)<sub>7</sub>, (dT)<sub>14</sub>, and (dT)<sub>21</sub> DNA probes are utilized to evaluate the ionic strength- and probe length-dependence of g32p binding. Absolute and normalized current densities are calculated for each sensor as it binds the g32p target. (*Top panel*) At both low (20 mM NaCl) and high (500 mM NaCl) salt conditions, the sensors demonstrate quantitative dependence on the DNA probe length. In general, increasing current densities is observed with decreasing probe length as a consequence of a more efficient electron transfer between the methylene blue and the gold electrode surface when the probe is shorter (hence, closer to the gold surface). Binding of the g32p target causes a decrease in the efficiency of this electron transfer, thus, results in a decrease in the measured percent signal changes. (*Bottom panel*) Plotting the normalized current densities as a function of g32p concentration clearly shows the quantitative dependence of the (dT)<sub>n</sub> E-DNA sensors both on ionic strength and DNA probe length (in contrast to using percent signal change). Specifically, at low salt concentrations (20 mM NaCl), the (dT)<sub>7</sub> sensor exhibits the weakest binding to g32p, while the (dT)<sub>21</sub> sensor shows the greatest affinity. At high salt concentrations, however, this observed trend is significantly

reversed. Here, the (dT)<sub>21</sub> sensor demonstrates weaker binding to g32p, which is presumably a consequence of the *cooperativity* exhibited by the g32 protein at *higher* salt concentrations,<sup>3</sup> as well as the *increased* electrostatic interactions that may have weakened the strong DNA-protein binding interactions initially observed at low salt concentrations.

## REFERENCES

- (1) Dill, K. A.; Bromberg, S. *Molecular Driving Forces: Statistical Thermodynamics in Chemistry and Biology* (Garland Science, New York). **2003**.
- (2) Josephs, E. A.; Ye, T. Nanoscale Spatial Distribution of Thiolated DNA on Model Nucleic Acid Sensor Surfaces. *ACS nano* **2013**, 7, 3653-3660.
- (3) Kowalczykowski, S. C.; Lonberg, N.; Newport, J. W.; von Hippel, P. H. Interactions of bacteriophage T4-coded gene 32 protein with nucleic acids. I. Characterization of the binding interactions. *J Mol Biol* **1981**, 145, 75-104.